Limitations of the observability of radio meteor head echoes in a forward scatter setup

Wolfgang Kaufmann [1]

During the maximum activity of the Quadrantids in 2018 a forward scatter radio observation failed to detect head echoes of this stream for more than one hour. A simulation of head echo Doppler shifts was performed on the basis of fixed receiver-transmitter-geometry with varying meteoroid trajectories in the height of 120–80 km. It could be shown that the ascertained head echo blackout coincided with a radiant position of the Quadrantids that resulted in trajectories producing very large Doppler shifts. From forward scatter radio observations it was found that the signal strength of a head echo declines rapidly with increasing Doppler shift. Simple forward scatter radio systems usually are too insensitive to detect head echoes Doppler shifts above a few kHz when meteoroid masses are small. This caused the blackout.

Received 2019 December 23

1 Introduction

The radio observation of meteors is possible via the reception of radio waves having been forward scattered off ionized meteor trails as well as off the small intense plasma region surrounding the meteoroids itself during their atmospheric passage between 140 and 70 km height. The latter scattering-type is called meteor head echo. Kero et al. (2008b) detected head echoes at aspect angles all the way out to 130° from the direction of meteoroid propagation (a further extension of the aspect angle was limited by the antenna pointing directions in their tristatic radar system). Thereby they found the radar cross section to be close to isotropic in the whole observable range, consistent with an essentially spherical target as first measured by Close et al. (2002).

The radio observation of such approximately isotropically scattering spheres theoretically should be possible from any position on the earth as long as they are above the horizon. The observability of head echoes is limited by the radar cross section of the meteoroid and the power of the transmitter in combination with the sensitivity of the receiver. The radar cross section mainly depends on the mass of the meteoroid, its velocity and height and on the frequency (Close et al., 2002).

On its flight a meteoroid shows a permanent changing radial velocity with respect to the observer (Kero et al., 2008a). In consequence the frequency of the head echo shows a continuously changing Doppler shift. E.g. during a radio observation of a fireball Rault et al. (2017) recorded an initial Doppler shift of 47 kHz continuously falling to zero Hz. From the radio observation of forward scattered head echoes the signal strengths of head echoes were found to decline rapidly with increasing Doppler shift (e.g. Kaufmann (2018), Fig. 2) So with smaller meteoroids only Doppler shifts of a few kHz can be observed with a basic receiving system. German (2020) showed in his simulation that there exists a number of trajectories resulting in very large Doppler shifts. These are far beyond the capability of a basic receiving system. So not all small meteoroids above the horizon deliver receivable head echoes. Their radio observability depends on the receiver-transmitter-trajectory geometry.

In the light of this finding the radio observation of the Quadrantids (QUA) 2018 were reexamined. During the maximum of activity not a single meteor head echo could be observed from Algermissen, Northern Germany for more than one hour. However trail reflections were present. No explanation has been found for this phenomenon so far. Now it may be explained by meteoroid trajectories resulting in unobservable large Doppler shifted frequencies. It is the aim of this paper to verify this hypothesis.

2 Material and Methods

A python script "MDopplerShift"[a] has been written to implement a bistatic radar model for calculating Doppler shifts. It was build on the thesis of Thomson (1985). The bistatic model bases on Cartesian coordinates. The origin of the coordinate system is coincident with the receiver position ($x = 0, y = 0, z = 0$). The transmitter is positioned at a distance D on the x-axis ($x = D, y = 0, z = 0$). The meteoroid is entering the scene anywhere in the space (x, y, z). Its bearing is indicated counterclockwise as angle between its forward direction and the receiver⇒transmitter direction (= baseline). Its inclination is specified as angle towards horizon. The meteoroid progress is stepwise calculated from its entry point. The Python script allows for the calculation of multiple trajectories from an entry point by automatically changing inclination and bearing in arbitrary steps. For further analysis the time-, x-, y-, z- and Doppler shift- data of the simulated trajectories were stored as csv-file. The further analysis was performed by a spread sheet program.

The radio registration of meteor reflections during the active period of the QUA 2018 took place in Algermissen, Northern Germany. The French radar-transmitter GRAVES was employed for forward scattering. It transmits a continuous rf-signal at a frequency of 143.050 MHz and illuminates a defined volume in the sky over southern France. A HB9CV-antenna, the SDR-receiver Funcube Dongle Pro+[b], the SDR-software

[1]Lindenweg 1e, 31191 Algermissen, Germany.
Email: contact@ars-electromagnetica.de

IMO bibcode WGN-481-kaufmann-observability
NASA-ADS bibcode 2020JIMO...48...12K

[a] http://www.ars-electromagnetica.de/robs/download.html
[b] http://www.funcubedongle.com/

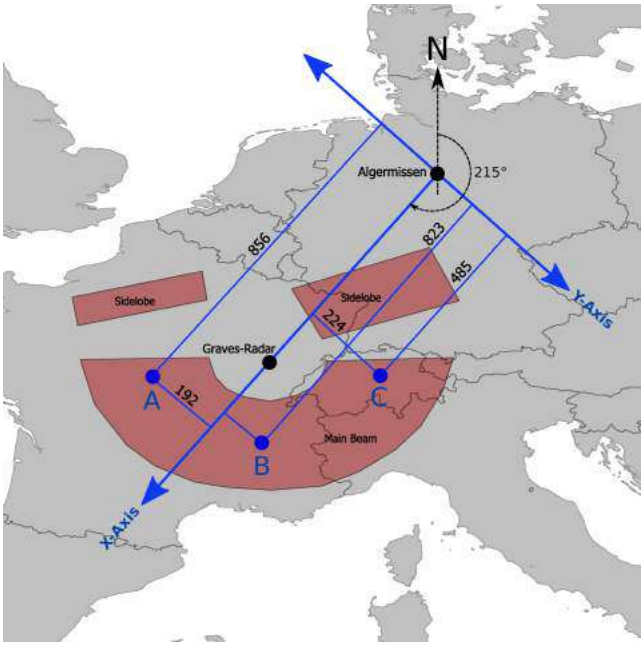

Figure 1 – Map of the receiver- and transmitter-positions. The GRAVES-radar illuminates a defined volume in the sky. A cross section in 100 km height is indicated (Kaufmann, 2018). Three meteoroid entry points, A-C, are chosen as representatives for all meteroroids entering the main beam. The x- and y-distances are indicated related to the receiver position. The distance between Algermissen and the transmitter is about 640 km. The azimuth of the receiver⇒transmitter baseline is about 215°. Map made with Natural Earth in the WGS 84 coordinate system.

SDR#[c] and the meteor-registration-software MeteorLogger[d] (Kaufmann, 2017) were used. The extraction of head echoes from the multitude of received signals and the computation of their frequency slopes was done by ProcessData[d]. Also ProcessData calculated the diurnal course of the QUA radiant in terms of azimuth (from north clockwise) and altitude from the given celestial coordinates at the time of maximum activity (Rendtel, 2017). For the head echo analysis the method of kernel density mapping was employed (Kaufmann, 2018), which is based on frequency slopes.

The trajectories of meteoroids originating from a radiant at azimuth, $AZ_{radiant}$, are orientated towards the observer and have therefore a reversed azimuth, $AZ_{meteoroid} = AZ_{radiant} + 180°$. The relation between the bearing of a meteoroid which is referenced to the baseline and its azimuth which is referenced to true North is $AZ_{meteoroid} = AZ_{baseline} - Bearing_{meteoroid} + 360$.

The extraction of head echoes of the QUA on base of the kernel density map was done by QGIS[e]. The head echo table can be imported in QGIS, using decimal date and log|slope| as x- and y-coordinates.

3 Results and Discussion

To get an idea which trajectories from which entry points can be recorded theoretically at Algermissen three representative entry points, A-C, were adopted in the main beam of GRAVES, see Figure 1. For each of this three entry points different trajectories were calculated by decreasing inclination from 0° to −90° in 5° steps and increasing bearing from 0° to 350° in 10° steps. Thereby progress of the meteoroids always was calculated in 100 ms steps. The geocentric velocity of incoming meteoroids was set to 40 km/s, the transmitter frequency to 143 050 000 Hz and the height z of the entry points to 120 km. The run time of the simulations was set to 5 s because of the finite extent of the illuminated sky volume. Figure 2 shows the graphical result of the simulation for entry point B. Obviously there exist a large number of trajectories that produce very large Doppler shifts in the given circumstances.

The existing, presumably numerous, back lobes of GRAVES were not taken into account, because their radiated power is much lower compared to the power of the main beam. Referred to the receiving system in use their contribution to the number of recorded head echoes is very small.

To adapt the outcome of the simulation to the capability of the used receiving system the data set was reduced to segments of trajectories which produce Doppler shifts running through zero Hz within a height of 120–80 km. From these segments the track points being closest to zero Hz Doppler shift were selected and their bearing/inclination-combinations were plotted, see Figure 3. The gaps between entry points A, B and C should be closed in real life by further entry points between A, B and C. So there remains a prominent gap centered around 200° bearing and a much smaller gap centered around 30° bearing. This would mean at Algermissen radio records at least do not include head echoes from meteoroids originating from southern radiants with an azimuth of around 195° and from northern radiants with an azimuth of approximately 5° if having a geocentric velocity of 40 km/s. The existence of such gaps were described by German (2020) as "no-go-zones."

Remarkable is that for a given bearing and inclination predominantly only one of the three entry point delivers head echoes with zero Doppler shifts (Figure 3). So for any bearing/inclination only a small part of the main beam reflects receivable head echoes towards Algermissen. This may additionally explain why the number of received head echoes in the radio measurements of Kaufmann (2018) were only about 10% of the number all signals. Hitherto this fraction was assumed to be only a matter of radar cross section of the incoming meteoroids.

The prediction of excluded head echo reception were verified by a radio observation of the head echoes of the Quadrantids 2018 (geocentric velocity about 41 km/s (Rendtel, 2014)). During the shower's maximum activity its radiant run through the above mentioned 5° azimuth gap. Figure 4 shows the kernel density map of all recorded head echoes from 2018 January 1 to 5. The QUA can be seen as prominent hot spot around January 4. Interestingly at the forecasted time of maximum activity January 3, 22^h UTC (Rendtel, 2017) over a span of more than one hour there was not a single head echo

[c] https://airspy.com/download/
[d] http://www.ars-electromagnetica.de/robs/download.html
[e] https://www.qgis.org

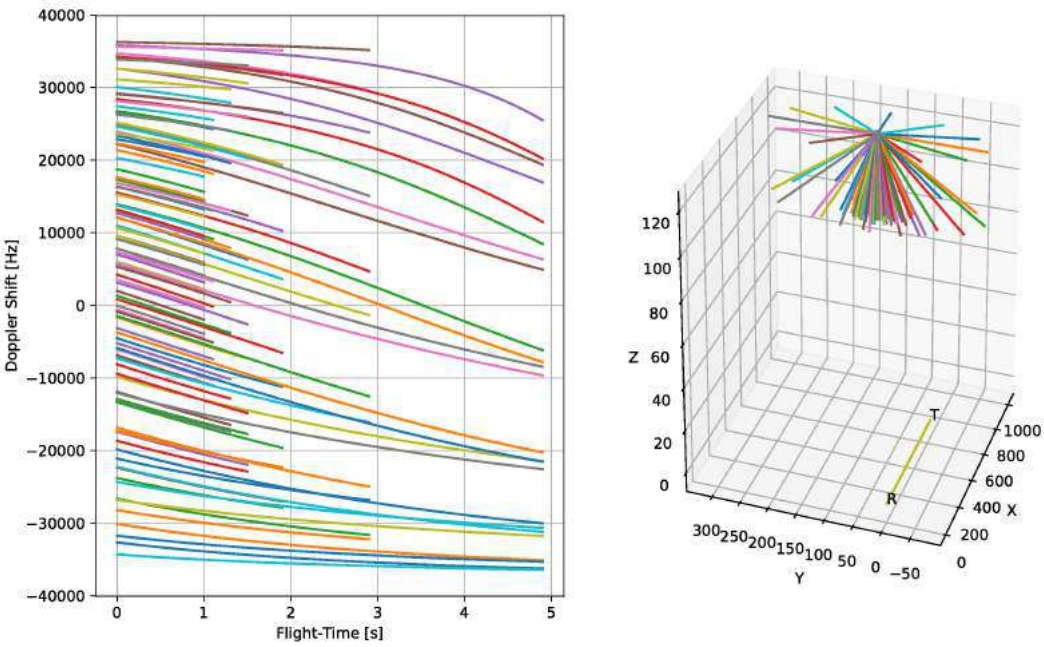

Figure 2 – The left plot is a graphical representation of the Doppler shifts produced by a meteoroid entering at point B (see Figure 1) with varied inclinations (10° steps) as well as bearings (30° steps). The right plot visualizes these different trajectories related to the receiver⇒transmitter baseline. The height is limited to a range of 120–80 km.

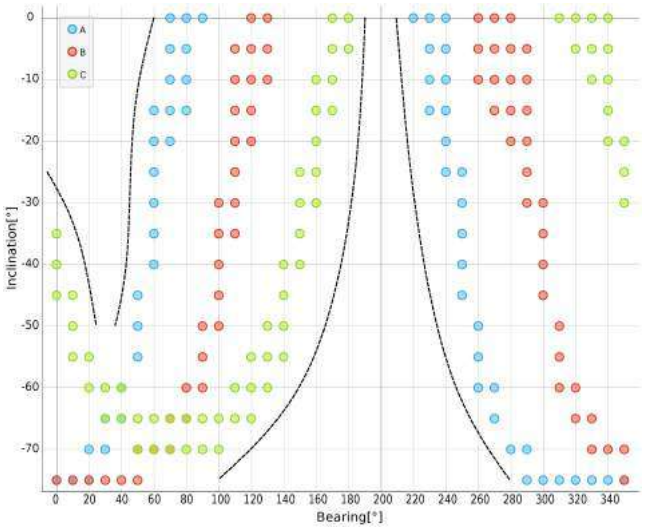

Figure 3 – Bearing-/inclination-combinations of track points close to zero Hz Doppler shift extracted from trajectories starting from the entry points A (blue), B (red) and C (green). Two gaps became apparent and were marked by dotted lines.

within the QUA hot spot registered. However trail reflections as well as head echoes of sporadic meteors were recorded. So this phenomenon was not due to a shutdown of the receiving system (as it was from January 3, 09^h–14^h UTC) or the very low altitude of the radiant at this point of time.

To analyse this further the QUA head echoes were extracted from the kernel density map by selecting all signals within the QUA hot spot. By this approach a small contribution of sporadic meteors of the apex source to the QUA could not be avoided in the period 03^h–06^h UTC because of the rather similar log|slopes| of both, see Figure 4. The QUA signals were summarized to hourly count rates (HCR). Mean hourly altitude is used for zenithal correction of the HCR [ZHR_r = HCR/ sin(altitude)] according to Rendtel et al. (2016). For a better comparability with Figure 3 the hourly means of azimuth and altitude of the QUA-radiant were converted to bearing and inclination of its meteoroids. Now the ZHR_r of the QUA head echoes were plotted in a bar chart together with the course of bearing and inclination of the QUA-meteoroids, see Figure 5. A progressive decline to 0 in the ZHR_r can be seen from 20^h–22^h UTC followed by a hesitant recovery of ZHR_r until 0^h. Within this time span the bearing moved from 30° down to 355° and inclination changed from −4° to −20°. Looking at Figure 3 all these combinations are lying completely within the gap centered around 30° bearing. The observed depletion of ZHR_r is not centered around 30° bearing but around 12°. However, considering that the sky illumination of GRAVES radar is an approximation derived from a few pieces of information and effects of meteoroid deceleration as well as curvature of the earth are not considered, the congruence between simulation prediction and real observation is remarkably well.

4 Conclusion

Although meteoroids are coated with an almost spherical plasma sheath from about 140 km down to 70 km height which should scatter incident radiation generally isotropically their head echoes are not observable in all case. Incoming meteoroids can have trajectories resulting in very large Doppler shifts in a forward scatter observation which make them unrecognisable to a basic receiving system. This effect not only modulates the number of recorded head echoes itself but also may prevent the coincident registration of a common meteoroid from different sites.

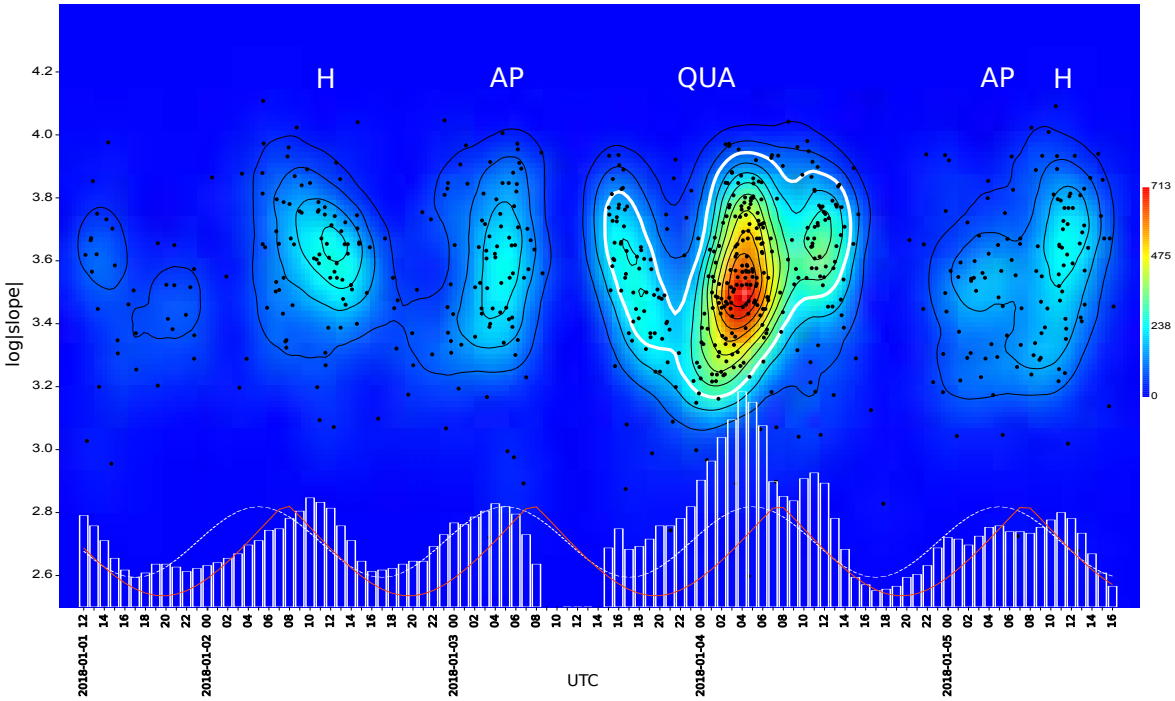

Figure 4 – Kernel density map of meteor head echoes recorded during the period 2018 January 1–5. Each dot represents the log|*slope*| of a head echo. The red line at the bottom depicts the relative course of the altitude of the radiant of the QUA. Also at the bottom the bar chart of the hourly count rates of all meteor reflections is inserted (max = 147). The white dotted line indicates the estimation of the amount of hourly sporadic meteors. The QUA can be seen as prominent hot spot. Also the helion (H) and apex (AP) source of sporadic meteors depict as weak hot spots.

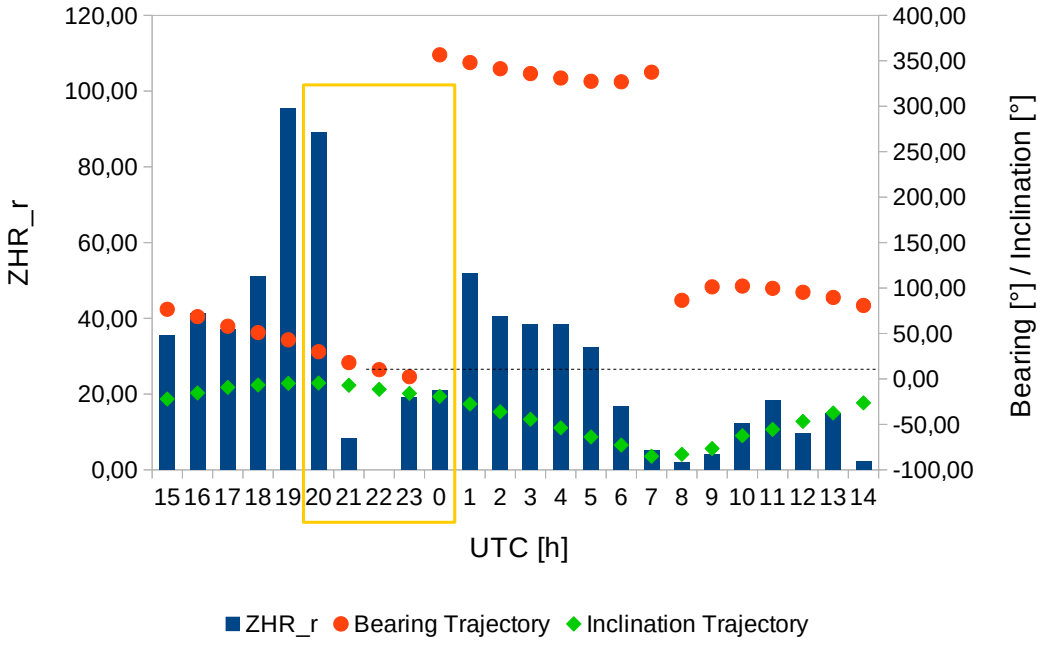

Figure 5 – Bar chart of the zenithal corrected hourly count rates of the QUA head echoes (ZHR_r) during the maximum activity in the period 2018 January 03–04. Bearing (right y-axis 0°–360°) and inclination (right y-axis −90°–0°) of the QUA-trajectories are indicated for the middle of each hour.

Acknowlegement

The author would like to thank M.T. German for inspiring him to this analysis, for intense discussions, valuable advice and helpful comments on the final draft.

References

Close S., Oppenheim M., Hunt S., and Dyrud L. (2002). "Scattering characteristics of high-resolution meteor head echoes detected at multiple frequencies". *J. Geophys. Res.*, **107:A10**, 1295.

German M. T. (2020). "A head echo Doppler model for assessment of meteoroid forward scatter characteristics". *WGN, Journal of the IMO*, **48:1**, 4–11.

Kaufmann W. (2017). "New radio meteor detecting and logging software". *WGN, Journal of the IMO*, **45:4**, 67–72.

Kaufmann W. (2018). "Visualizing meteor streams by radio forward scattering on the basis of meteor head echoes". *WGN, Journal of the IMO*, **46:1**, 39–44.

Kero J., Szasz C., Pellinen-Wannberg A., Wannberg G., Westman A., and Meisel D. D. (2008a). "Determination of meteoroid physical properties from tristatic radar observations". *Ann. Geophys.*, **26**, 2217–2228.

Kero J., Szasz C., Wannberg G., Pellinen-Wannberg A., and Westman A. (2008b). "On the meteoric head echo radar cross section angular dependence". *Geophysical Research Letters*, **35**, L07101. doi:10.1029/2008GL033402.

Rault J.-L., Birlan M., Blanpain C., Bouley S., Caminade S., Colas F., Gattacceca J., Jeanne S., Lecubin J., Malgoyre A., Marmo C., Vaubaillon J., Vernazza P., and Zanda B. (2017). "Fine-scale observations of the doppler frequency shifts affecting meteor head radio echoes". In Gyssens M. and Rault J.-L., editors, *Proceedings of the International Meteor Conference, Petnica, Serbia 21-24 September, 2017*. IMO, pages 103–106.

Rendtel J. (2014). *Meteor Shower Workbook 2014*. International Meteor Organization, Potsdam.

Rendtel J. (2017). "2018 Meteor Shower Calendar". International Meteor Organization. IMO_INFO(2-17).

Rendtel J., Ogawa H., and Sugimoto H. (2016). "Quadrantids 2016: observations of a short pre-maximum peak". *WGN, the Journal of the IMO*, **44:4**, 101–107.

Thomson W. P. (1985). "Airborne bistatic radar limitations and sample calculations". Master's thesis, Air Force Institute of Technology, Ohio.

Handling Editor: Jean-Louis Rault